DMD5447

In vitro inhibition of UDP-glucuronosyltransferases by atazanavir and other HIV protease inhibitors and the relationship of this property to in vivo bilirubin glucuronidation

Donglu Zhang, Theodore J Chando, Donald W Everett, Christopher J Patten, Shangara S Dehal, and W Griffith Humphreys

Pharmaceutical Candidate Optimization, Pharmaceutical Research Institute, Bristol-Myers Squibb, Princeton, NJ 08543 (DZ, TJC, DWE, WGH);

Gentest, BD Biosciences, Boston, MA 01801 (CJP and SSD)

1

DMD5447

Running title: Inhibition of bilirubin glucuronidation by HIV protease inhibitors

Address correspondence to:

Donglu Zhang, Ph.D.

Pharmaceutical Candidate Optimization,

Bristol-Myers Squibb, P.O. BOX 4000,

Princeton, NJ 08543.

Phone: 609-252-5582.

Email: Donglu.Zhang@BMS.com

[1]Abbreviations used: AUC, area under the plasma drug concentration vs time curve; HLM, human liver microsomes; HIV, human immunodeficiency virus; UDPGA, uridine 5'-diphospho-glucuronic acid; UGT, uridine 5'-diphospho-glucuronosyltransferase

Text pages (including references): 27

# of table: 5

# of figures: 6

# of references: 45

# of words in abstract: 210

# of words in introduction: 700

# of words in discussion: 1650

DMD5447

ABSTRACT

Several HIV protease inhibitors, including atazanavir, indinavir, lopinavir, nelfinavir, ritonavir, and saquinavir, were tested for their potential to inhibit UGT activity. Experiments were performed with human cDNA-expressed enzymes (UGT1A1, 1A3, 1A4, 1A6, 1A9, and 2B7) as well as human liver microsomes. All of the protease inhibitors tested were inhibitors of UGT1A1, UGT1A3, and UGT1A4 with IC_{50} values that ranged from 2 to 87 microM. The IC_{50} values found for all compounds for UGT1A6, 1A9, and 2B7 were >100 microM. The inhibition (IC_{50}) of UGT1A1 was similar when tested against the human cDNA-expressed enzyme or human liver microsomes for atazanavir, indinavir, and saquinavir (2.4, 87, and 7.3 microM vs. 2.5, 68, and 5.0 microM, respectively). By analysis of the double-reciprocal plots of bilirubin glucuronidation activities at different bilirubin concentrations in the presence of fixed concentrations of inhibitors, the UGT1A1 inhibition by atazanavir and indinavir was demonstrated to follow a linear-mixed type inhibition mechanism (K_i = 1.9 and 47.9 microM, respectively). These results suggest that a direct inhibition of UGT1A1 mediated bilirubin glucuronidation may provide a mechanism for the reversible hyperbilirubinemia associated with administration of atazanavir as well as indinavir. An in vitro-in vivo scaling with $[I]/K_i$ predicts that atazanavir and indinavir are more likely to induce hyperbilirubinemia than other HIV protease inhibitors studied when a free C_{max} drug concentration was used. Current study provides a unique example of in vitro-in vivo correlation for an endogenous UGT mediated metabolic pathway.

3

DMD5447

Introduction

The HIV protease is an essential enzyme that cuts the viral gag-pol polyprotein into its functional subunits. Atazanavir, indinavir, saquinavir, lopinavir, ritonavir, and nelfinavir are HIV protease inhibitors. The structures of these HIV protease inhibitors are shown in Figure 1. Different from atazanavir, which is an azapeptide protease inhibitor (Goldsmith and Perry, 2003), other listed HIV protease inhibitors are peptidomimetics sharing the same structural determinant, i.e. a hydroxyethylene or a hydroxyethylamine moiety, which makes them nonscissile HIV protease substrate analogs. These HIV protease inhibitors are metabolized primarily by hepatic CYP3A enzymes and they are also inhibitors of CYP3A enzymes (Flexner, 2000; Goldsmith and Perry, 2003; de Maat et al., 2003, Ernest et al., 2005). All of these HIV protease inhibitors have a high protein binding (>98%), except indinavir and atazanavir which have a protein binding of 60 and 86%, respectively. Most of the HIV protease inhibitors are bound to α1-acid glycoprotein instead of albumins (de Maat et al., 2003). There are no literature reports indicating that HIV protease inhibitors are good substrates for human UGT enzymes, although there is evidence to support indinavir as a substrate of UGTs (Balani et al., 1996).

Glucuronidation represents a major pathway for the elimination of a vast number of endogenous chemicals and xenobiotics. UGT1A1 is the only known human UGT to glucuronidate bilirubin (Burchell et al., 1995). In addition to bilirubin glucuronidation, a critical physiological metabolic reaction, UGT1A1 also catalyzes glucuronidation of carboxylic acid containing drugs such as

4

DMD5447

fluoroquinolones moxifloxacin and sitafloxacin as well as non-steroidal anti-inflammatory drugs sulindac, sulindac sulfone, and indomethacin (Kuehl et al., 2005; Tachibana et al., 2005). UGT2B7 is a very important enzyme for the glucuronidation of many drugs (Williams et al., 2004).

Bilirubin is a waste product (approximately 4 mg/kg/day produced by normal subjects) mainly derived from the degradation of hemoglobin from senescent red blood cells (Berk et al., 1974; Berk et al., 1979). Unconjugated bilirubin is highly bound to albumin and can lead to toxicities if the bilirubin:albumin molar ratio exceeds 1:1. Several steps are involved for elimination of bilirubin. Unconjugated bilirubin in the circulation is likely transported to the liver by the liver specific organic anion uptake transporting polypeptide OATP1B1 (Briz et al., 2003). UGT1A1 catalyzes glucuronidation of bilirubin at one or both of the two-propionic acid groups with glucuronic acid, which is required for the following elimination via the biliary transporter MRP2 (Kamisako et al., 2000). In humans, the glucuronidication of bilirubin is carried out exclusively by UGT1A1 with an apparent K_m value of <10 μM, which is a lower value than most of other glucuronidation reactions (Williams et al., 2004; Luukkanen et al., 2005). The glucuronidated bilirubin may also be carried back to sinusodial blood by MRP3 if biliary excretion pathways (e.g. MRP2) are impaired (Keppler and Konig, 2000). There are a number of mutations in the UGT1A1 gene that have been described that lead to decreased UGT1A1 activities and increased levels of bilirubin, i.e., patients with Crigler-Nijjar and Gilbert syndromes (Miners et al., 2002; Zucker et al., 2001). Crigler-Nijjar and Gilbert syndromes result from genetic

polymorphisms in the UGT1A1 coding region and/or promoter leading to an approximately 90% and 40% reduction in bilirubin clearance, respectively (Tukey and Strassburg, 2000). Crigler-Nijjar syndrome is rare, but approximately 10% of the US population has the Gilbert polymorphism. Dubin-Johnson syndrome results from the polymorphism in MRP2 transporter that associates with conjugated hyperbilirubinemia (Tukey and Strassburg, 2000).

Inhibition of bilirubin glucuronidation enzyme UGT1A1 would have potential to produce elevated unconjugated bilirubin concentration in the circulation (Brierley and Burchell, 1993). Unconjugated hyperbilirubinemia after administration of indinavir was attributed to direct inhibition of UGT1A1 by this drug (Zucker et al., 2001). Unconjugated hyperbilirubinemia has also been observed as an adverse event of atazanavir administration, however, this measurable increase is not clinically significant and the therapy stop was not needed since the concentrations of unconjugated bilirubin never reached to a toxic level (Goldsmith and Perry, 2003). The unconjugated hyperbilirubinemia associated with atazanavir administration was rapidly reversible, suggesting that the serum bilirubin increase is a specific metabolic phenomenon and not a reflection of cellular injury (Goldsmith and Perry, 2003). To investigate if there is a common mechanism for the unconjugated hyperbilirubinemia associated with administration of indinavir or atazanavir and to compare to other HIV protease inhibitors, atazanavir along with several other HIV protease inhibitors were tested as inhibitors of UGT1A1 and several other UGT enzymes.

Materials and Methods

Materials. Atazanavir (BMS-232632) was prepared at Bristol-Myers Squibb. Other test substances, including indinavir, saquinavir, lopinavir, ritonavir, and nelfinavir, were commercially available. A stock solution of the test substance was prepared in 100% methanol at a concentration of 10 or 30 mM on the day of the experiment. Additional dilutions were made in methanol for each of the final inhibitor concentrations. The solvent concentrations were constant (1% final) for all incubations with and without the test substance. Human UGT supersomes™ (membranes of insect cells transfected with baculovirus containing human cDNA of UGTs or microsomes of lymphoblast cells heterologously expressing human cDNA of UGT1A1) and human liver microsomes (pooled from 20 subjects) were from BD Gentest (Woburn, MA). Bilirubin, β-estradiol, 17β-estradiol 3-glucuronide, trifluoperazine, 7-hydroxy-4-trifluoromethylcoumarin, 7-hydroxy-4-trifluoromethylcoumarin glucuronide, 2-hydroxy-estradiol, hecogenin, propofol, naphthol, and eugenol were purchased from Sigma Chemical Co. (St. Louis, MO). All other chemicals were of reagent grade or better.

Incubation conditions for UGT1A1. Incubations were conducted at 37°C in a final volume of 0.2 ml in 50 mM sodium citrate buffer (pH 7.5) with 2 mM UDPGA, 25 µg/ml alamethicin, 10 mM MgCl$_2$, and bilirubin. Bilirubin was dissolved in 100% DMSO and added to the incubation to the desired final bilirubin concentration. The final microsomal protein concentration was generally 0.125-1 mg/ml. Reactions were initiated by addition of the UGT enzyme. Termination of the reaction was achieved by the addition of 0.2 ml ethanol

containing 2% ascorbic acid. Samples were centrifuged for 10 min (10,000xg) to remove protein, and 140 or 150 µl of supernatant was injected onto HPLC. Reactions were carried out in reduced light in amber Eppendorf tubes due to the light sensitivity of bilirubin. Control incubations contained all the assay components minus the UDPGA cofactor. Under these conditions, percent metabolism was less than 10%. The recovery of the glucuronides in the supernatant was quantitative as determined by extensive extraction of the protein pellet.

For the time course experiment, incubations containing 1.25 mg/ml protein and 10 µM bilirubin were terminated after 10, 20, 30, 40 and 50 min. For the protein concentration dependence experiment, the final protein concentrations were 0.33, 1.0, 1.67, and 2.3 mg/ml in incubations containing 50 µM bilirubin and the reactions were terminated after 40 min. For substrate concentration-dependent experiments, the bilirubin concentrations were 2, 5, 10, 20, 30, 40, and 60 µM in incubations containing a final protein concentration of 1.67 mg/ml and the reactions were terminated after 35 min.

Incubation conditions with other UGT enzymes. Table 1 shows the substrates and inhibitors used for assaying UGT activities. In general, incubation mixtures contained 50 mM buffer, 2 mM UDPGA, 10 mM $MgCl_2$, substrate, and enzyme proteins in a final volume of 0.2 ml. Following incubations, the reactions were terminated by adding 0.05-0.2 ml of 6% acetic acid in acetonitrile. After removal of protein by centrifugation for 10 min (10,000xg), the supernatant was injected onto HPLC.

Determination of IC$_{50}$ and K$_i$. Incubations were performed in duplicate for IC$_{50}$ determinations. The test substance concentrations were 0.03, 0.1, 0.3, 1, 3, 10, 30, 100, and 300 µM. For atazanavir, the final bilirubin concentration was 8 µM, the assay time was 40 min, and the final protein concentration was 1 mg/ml. For indinavir, the final bilirubin concentration was 5 µM, the assay time was 35 min, and the final protein concentration was 1 mg/ml.

Incubations were performed in triplicate for K$_i$ determinations. For assays with atazanavir, the bilirubin concentrations were 3, 6, 9, 12, and 15 µM and the atazanavir concentrations were 0, 3, 6, and 12 µM. Incubations contained 1 mg/ml protein and were run for 38 min. For indinavir, the bilirubin concentrations were 2, 5, 10, and 20 µM and the indinavir concentrations were 0, 50, 100, 150, and 250 µM. Incubations contained 1 mg/ml protein and were run for 35 min.

HPLC Method. For analyzing bilirubin glucuronidation incubations, HPLC conditions consisted of two mobile phases: A) 0.1% TFA in H$_2$O and B) 0.1% TFA in 100% acetonitrile. Initial conditions consisted of 90% A and 10% B. Bilirubin glucuronides were separated at 45°C by a linear increase of solvent B from 10% to 100% over 25 min, and held at 100% B for 5 min before returning to initial conditions. The flow rate was 1 ml/min. The HPLC column was a C18 LiChrospher (Merck, 5 µ, 4 x 250 mm). Bilirubin and glucuronide metabolites were detected at 450 nm. In the presence of expressed UGT1A1 and UDPGA, bilirubin was glucuronidated to both the cluster of four peaks for mono-glucuronides (15.4-16.6 min) and a di-glucuronide product (12.5 min) (Figures 2 and 3). The retention times and number of bilirubin glucuronide isomers

(cis/trans and positional isomers) detected in the current study is in good agreement with a previous report (Odell et al., 1990). Bilirubin glucuronide peaks were quantitated using bilirubin in a buffer (Solvent A and B, 50:50, v/v) as a standard because bilirubin glucuronide metabolites are not commercially available. The sum of the peak area for the mono- and di-glucuronides, including two minor isomers, were used for quantitation of total bilirubin glucuronidation.

The supernatant of UGT1A3 reaction was injected on a 4.6 x 250 mm, 5 μ, C18 Zorbax HPLC column (Agilent Technologies, Wilmington, DE) and separated at 45°C at a flow rate of 1 ml/min with a mobile phase of 10% methanol (A), 100% methanol (B) and 1 mM perchloric acid in 30% acetonitrile in water (C). Initial conditions were 85% A and 15% C. Mobile phase B was increased linearly from 0% to 85% over 20 min while keeping C at 15% and held at 85% B for 2 min before returning to initial conditions. The column was allowed to equilibrate for 11 min before the next injection. The absorbance of the product was measured at 280 nm and the response was quantitated by comparison to a standard curve of 17β-estradiol 3-glucuronide.

The supernatant of UGT1A6, UGT1A9 and UGT2B7 reactions was injected on a 4.6 x 250 mm, 5 μ, C18 Zorbax HPLC column and separated at 45°C at a flow rate of 1 ml/min with a mobile phase of 10% methanol (A), 100% methanol (B) and 1 mM perchloric acid in 30% acetonitrile in water (C). Initial conditions were 80% A, 10% B and 10% C. Mobile phase B was increased linearly from 10% to 90% over 15 min while keeping C at 10% and returned to initial conditions over 10 sec. The column was allowed to equilibrate for 15 min before the next

injection. The absorbance of the product 4-trifluoromethyl-7-hydroxycoumarin glucuronide was measured at 325 nm and the response was quantitated by comparison to a standard curve of 4-trifluoromethyl-7-hydroxycoumarin glucuronide.

The supernatant from the UGT1A4 and trifluoperazine reaction was injected on a 4.6 x 250 mm, 5 μ, C18 Zorbax HPLC column and separated at 45°C with a mobile phase of 0.1% trifluoroacetic acid in water (A) and 0.1% trifluoroacetic acid in acetonitrile (B) at a flow rate of 1 ml/min. Initial conditions consisted of 70% A and 30% B. Mobile phase B was increased to 51% by a linear gradient over 14 min and then returned to initial conditions over 10 sec and the column was re-equilibrated for 10 min before the next injection. The absorbance of the product was measured at 256 nm and the response was quantitated by comparison to a standard curve of trifluoperazine. The parent trifluoperazine was used as the quantitation standard because the authentic metabolite trifluoperazine glucuronide was not available commercially.

Data Analysis. The IC_{50} value was determined by linear interpolation. The mechanism of inhibition (i.e. competitive, non-competitive, uncompetitive, or mixed-type) was determined from 1/V versus 1/S plots at each inhibitor concentration (Segel, 1993). The apparent K_i was determined from the x-intercept of a re-plot of the mean slopes of the double reciprocal plot versus [I] (test substance concentration) (Segel, 1993). Likewise, the apparent αKi was determined from the x-intercept of the mean y-intercepts of the double reciprocal plot versus [I] (Segel, 1993). Graphs were created and linear regression and

non-linear regression calculations were carried out using SigmaPlot® software (SPSS Inc, Chicago, IL). Statistical analysis (mean, standard deviation, and co-variance (CV)) were determined using Microsoft Excel software.

Rowland and Matin (1973) developed an equation, $AUC_i/AUC = 1 + [I]/K_i$, to predict the increase in drug AUC for oral or intravenous drugs caused by a competitive inhibitor, where [I] is the inhibitor concentration at the enzyme site that is available to the metabolism enzyme and K_i is the in vitro inhibition constant (Ito et al., 1998; Yao and Levy, 2002). This approach is only valid when a drug's clearance is mainly mediated by one metabolic enzyme. This in vitro-in vivo scaling approach is also applicable to non-competitive inhibition when the substrate concentration is much smaller than its K_m, which is true for most clinical situations (Ito et al., 1998). The inhibition of bilirubin glucuronidation by HIV protease inhibitors would not be mechanism-based since they are not even UGT enzyme substrates; it is highly unlikely to be uncompetitive since very few of examples of uncompetitive inhibition are known; and it is likely that the inhibition follows a competitive, non-competitive, or a mixed model. The apparent K_i values for competitive portion of the inhibition were determined for atazanavir and indinavir. When the assays are performed at a substrate concentration equivalent to the K_m value, $K_i = 1/2 \, IC_{50}$ for competitive inhibition and $K_i = IC_{50}$ for non-competitive inhibition. The inhibition type has not been elucidated for lopinavir, nelfinavir, ritonavir, and saquinavir and so $K_i = 1/2 \, IC_{50}$ for competitive inhibition was used for these inhibitors. Using a competitive inhibition model is a

12

conservative approach to minimize false-negative predictions since the lowest possible estimate of K_i is used.

Results

The glucuronidation of bilirubin was shown to be linear for at least 50 min under the incubation conditions used. The rate of glucuronidation increased linearly with increasing amounts of proteins up to 2.3 mg/ml (the highest protein concentration used). Bilirubin glucuronidation appeared to follow simple Michaelis-Menten kinetics. A non-linear regression/direct plot analysis resulted in an apparent K_m and V_{max} of 4 μM and 80 pmol/min/mg protein, respectively. The apparent K_m value reported in this study was in good agreement with a previous study that demonstrated an apparent K_m of about 5 μM for bilirubin glucuronidation by recombinant UGT1A1 (Ciotti et al., 1998). Other studies have reported a higher K_m value (25 μM) for bilirubin glucuronidation by the expressed UGT1A1 enzyme (Senafi et al., 1994). The reason for this discrepancy is not known, but is likely due to differences in the cell line and assay methodology. Under the same assay conditions, pooled human liver microsomes demonstrated an apparent K_m value of 6.2 μM and a V_{max} of 1000 pmol/min/mg protein for bilirubin glucuronidation (data not shown). The apparent K_m values for the bilirubin glucuronidation was similar between the human cDNA-expressed UGT1A1 and the human liver microsomes.

Table 2 shows the IC_{50} values found for the inhibition of several UGT enzymes expressed in baculovirus-infected insect cells by the HIV inhibitors atazanavir, indinavir, saquinavir, lopinavir, ritonavir, and nelfinavir. Human UGT1A1 was

13

inhibited by all the protease inhibitors tested, with a potency rank of atazanavir > lopinavir ~ nelfinavir ~ saquinavir > ritonavir > indinavir. The inhibition potency rank orders are different for UGT1A3 and UGT1A4. For UGT1A3, lopinavir, saquinavir, ritonavir and atazanavir had a similar inhibition potential and nelfinavir and indinavir showed a lower inhibition potential. For UGT1A4, the inhibition rank order follows ritonavir > lopinavir ~ saquinavir > atazanavir ~ nelfinavir > indinavir. No significant inhibition of UGT1A4 by indinavir and of UGT1A6, 1A9 or 2B7 was observed by any of these HIV protease inhibitors.

The inhibition of bilirubin glucuronidation was further investigated in both human liver microsomes and cDNA-expressed UGT1A1 in lymphoblast cells by selected HIV protease inhibitors. Table 3 shows the IC_{50} and estimated K_i values for inhibition of bilirubin glucuronidation by these inhibitors. Indinavir demonstrated the highest IC_{50} value and atazanavir the lowest IC_{50} value in human liver microsomes and expressed UGT1A1. The IC_{50} values in human liver microsomes were similar to those with expressed UGT1A1 for atazanavir, indinavir, and saquinavir. Nelfinavir demonstrated a significantly lower IC_{50} values in human liver microsomes than in the expressed UGT1A1, which was confirmed with additional experiments (data not shown).

Atazanavir was shown to be an inhibitor of bilirubin glucuronidation with an IC_{50} value of 2.4 µM at a bilirubin concentration of 8 µM. For the K_i determination, a 4 x 5 inhibitor/bilirubin concentration matrix was chosen based on the IC_{50} value of atazanavir, and the apparent K_m value for UGT1A1-dependent bilirubin glucuronidation. Double reciprocal plots of the substrate concentration data (1/V

14

vs 1/S) in the presence of fixed concentrations of atazanavir show that both the slopes and the y-intercepts increase with increasing inhibitor concentrations, suggesting that atazanavir inhibits bilirubin glucuronidation by a "mixed-type" mechanism (Figure 4A) (Segel, 1993). The Dixon plot was not able to distinguish between a competitive and a "mixed-type" inhibition (Figure 5). Re-plotting the slopes of the Dixon plots produced a straight line that does not pass through the origin, consistent with a "mixed-type" inhibition mechanism (data not shown). The re-plot of the slope of the double reciprocal plots vs. [I] produced a straight line with x-intercept of 1.9 µM, which is equal to the apparent K_i value (Figure 4B) (Segel, 1993). αK_i, a measure of the affinity of ES for I, was 16.4 µM, which was determined from the x-intercept of the re-plot of the y-intercept values of the double reciprocal plot. In conclusion, the results of this study demonstrate that atazanavir inhibits recombinant UGT1A1 via a linear "mixed-type" mechanism, i.e., both the apparent K_m and V_{max} are related in an inverse manner with a K_i value of 1.9 µM (Table 4).

Indinavir was shown to inhibit bilirubin glucuronidation in recombinant UGT1A1, with an IC_{50} value of 87 µM at a final bilirubin concentration of 5 µM. For the K_i determination, a 5 x 4 inhibitor/bilirubin concentration matrix was chosen based on the IC_{50} value, and the apparent K_m value for UGT1A1-dependent bilirubin glucuronidation. The 1/V vs 1/S double reciprocal plots in the presence of fixed concentrations of indinavir show that the slope of the lines increased with increasing inhibitor concentrations, suggesting a competitive mechanism of inhibition (Figure 6A). The lines of the double-reciprocal plots intersected slightly

to the left of the y-axis, suggesting that indinavir also decreased the V_{max} of bilirubin glucuronidation. This result suggests that indinavir inhibits bilirubin glucuronidation by a near-competitive "mixed-type" mechanism. The re-plot of the slope gave a K_i value of 47.9 µM (Figure 6B) (Segel, 1993). αK_i was 1317 µM. In conclusion, the results of this study demonstrate that indinavir inhibits recombinant UGT1A1 via a linear "mixed-type" mechanism with a moderately low apparent K_i value of 47.9 µM (Table 4).

Table 5 shows the relationship of in vitro UGT1A1 inhibition to observations of hyperbilirubinemia by the HIV protease inhibitors investigated. To correlate the apparent in vitro UGT1A1 inhibition data with the in vivo elevation of unconjugated bilirubin, the in vitro-in vivo scaling was attempted based on the equation $AUC_i/AUC = 1 + [I]/K_i$ (Rowland and Matin, 1973). The C_{max}, C_{min}, and the corresponding free drug concentrations were used for [I] and K_i values were determined for atazanavir and indinavir and were estimated from IC_{50} values for other drugs with a assumption of a competitive inhibition. There is no general correlation when C_{max} or C_{min} were used directly and the C_{max}/K_i scaling produced false positive for lopinavir, ritonavir, and nelfinavir. However, when a free or unbound concentration, $C_{max,u}$, was used, the intrinsic fraction of UGT1A1 that can be inhibited ($[I]/K_i$) was >0.1 for atazanavir and indinavir, which are know to produce hyperbilirubinemia in some patients and were <0.1 for saquinavir, lopinavir, ritonavir, and nelfinavir, which are not known to produce hyperbilirubinemia. Saquinavir, lopinavir, ritonavir, and nelfinavir have a K_i value of about 5-10 fold lower than indinavir, but their unbound fractions were more

16

than 20 fold lower than indinavir, resulting in lower $C_{max,u}/K_i$ values than indinavir. $C_{min,u}/K_i$ values were too low to be meaningful.

Discussion

Our results have demonstrated that atazanavir, indinavir, saquinavir, lopinavir, ritonavir, and nelfinavir inhibited the enzyme activity of UGT1A1, UGT1A3, and UGT1A4, and had little effect on UGT1A6, UGT1A9, and UGT2B7. This selectivity profile is not unexpected based on amino acid sequence analysis of the UGT enzymes (Tukey and Strassburg, 2000). UGT1A3 and UGT1A4 share 93% identity of amino acid sequences, and they both share 71% homology with UGT1A1. The amino acid sequence homology is decreased to 66-67% with UGT1A6 and UGT1A9, and to 41% with UGT2B7. The close amino acid sequences between UGT1A1, UGT1A3 and UGT1A4 may generate a similar 3-dimensional structure for binding to these structurally related HIV protease inhibitors. UGT1A3 and UGT1A4 catalyze the glucuronidation of important endogenous substances including primary, secondary, and tertiary amines and steroids (Green et al., 1998). Although implications of the in vitro inhibition of UGT1A3 and UGT1A4 are currently not known, our inhibition data suggest that HIV protease inhibitors would be useful inhibitors to study UGT1A3 and UGT1A4 enzymes. The following discussion will focus on inhibition of UGT1A1 and the subsequent effects on bilirubin glucuronidation.

The most abundant naturally occurring bilirubin structure is designated bilirubin-4Z,15Z-IXa. Its stereochemical configuration favors formation of internal hydrogen bonds between the propionic acid chains and the polar -NH-CO- and

=NH groups (lactam and imino groups) on the opposite half of the molecule. The hydrogen bonds actually fix the molecule in a rigid 3-dimensional configuration that blocks exposure of the polar groups and leads to bilirubin's hydrophobic properties (Berk et al., 1974). The fact that bilirubin is also a potent inhibitor of HIV-1 protease (McPhee et al., 1996) suggests that these HIV protease inhibitors may share structural similarities to bilirubin. Although these protease inhibitors are poor substrates for human UGT enzymes, they do seem to bind to the substrate binding site of UGT1A1 since our data support that atazanavir and indinavir were at least partially competitive inhibitors of UGT1A1.

The exposure of a drug may be increased if its major clearance pathways are inhibited by a second compound. Drug-drug interactions through inhibition of CYP or transporter mediated clearance are a major concern because they can lead to dramatic alteration of a drug's efficacy or safety profiles. In contrast to CYP-mediated pathways, for drugs primarily cleared by glucuronidation there are only a few reports describing clinically relevant drug interactions through inhibition of UGT enzymes and the increase in drug exposures are typically less than 2-fold in the presence of UGT inhibitors (Liston et al., 2001; Boase and Miners, 2002; Lin and Wong, 2002; Williams et al., 2004). The less than 2-fold exposure increase for drugs primarily cleared by glucuronidation has been attributed to the relatively high K_m values for UGT substrates compared with liver drug concentrations at therapeutic doses, and the fact that multiple UGT enzymes are often involved in the metabolism of a single substrate (Williams et al., 2004; Kiang et al., 2005).

DMD5447

The inhibition of an endogenous metabolic pathway such as UGT1A1-mediated bilirubin glucuronidation by indinavir and atazanavir can be viewed mechanistically as analogous to a drug-drug interaction. Although most of the drugs that use enzymes as disease targets inhibit formation of enzyme products for their pharmacological activities such as the inhibition of cleavage of the HIV gal-pol polyprotein into the functional subunits by the protease inhibitors, very few cases of inhibition of endogenous metabolic pathways have been reported to associate with accumulation of the enzyme substrates leading to toxicities. Drugs have the potential to inhibit a metabolic reaction leading to elevation of the level of the endogenous substance. The hyperbilirubinemia associated with administration of indinavir and atazanavir may thus be reasonably expected to be mediated by inhibition of UGT1A1 as described herein. Consistent with this mechanism, unconjugated serum hyperbilirubin was significantly higher in Gilbert patients treated with either atazanavir or indinavir compared to untreated Gilbert patients who have a lower base levels of UGT1A1 activities than normal subjects (O'Mara et al., 2000; Zucker et al., 2001). The unconjugated hyperbilirubinemia associated with administration of indinavir and atazanavir was rapidly reversible and asymptomatic, and not associated with elevations of hepatic enzymes such as alanine transaminase or aspartate transaminase (Sulkowski, 2004). In addition to UGT1A1 inhibition, indinavir was recently shown to inhibit OATP1B1, a hepatic uptake transporter for bilirubin, which provides an additional potential mechanism for indinavir-induced hyperbilirubinemia (Campbell et al., 2005). In the same report, saquinavir did not inhibit OATP1B1, which correlates with the

19

fact that saquinavir does not produce hyperbilirubinemia. It is not known whether atazanavir inhibits hepatic OATP1B1.

The [I]/K_i approach has been used to predict or correlate many in vivo drug-drug interactions mediated by CYP enzymes with the use of in vitro K_i data and some measure of in vivo inhibitor concentrations (Ito et al., 1998; Ito et al., 2005; Thummel and Wilkinson, 1998; Bertz and Grannerman, 1997; Venkatakrishnan et al., 2001; Rodrigues et al., 2001; Galetin et al., 2005). The prediction of hyperbilirubinemia based upon the [I]/K_i approach, where [I] was the total plasma C_{max} value of the HIV protease inhibitor, gave results that did not match the clinical observations with these drugs (Table 5). Although previous reports (Ito et al., 2004, 2005) have shown that total inhibitor concentrations together with in vitro K_i values resulted in more positive and negative predictions, as well as less false positive and negatives, for in vivo drug-drug interactions involving CYP3A4, CYP2D6, and CYP2C9, this may not hold true for the UGT enzyme system. Indeed, the in vitro-in vivo scaling using [I]/K_i with the unbound C_{max} did predict that atazanavir and indinavir are more likely to produce hyperbilirubinemia than saquinavir, lopinavir, ritonavir, and nelfinavir (Table 5). Indinavir has the highest unbound plasma concentration and is more likely to produce hyperbilirubinemia than saquinavir, lopinavir, ritonavir, and nelfinavir, although indinavir has a higher K_i value. Although the [I]/K_i with the unbound drug did rank order the compounds correctly, it did not quantitatively predict the several fold elevation of unconjugated bilirubin associated with administration of atazanavir and indinavir ([I]/K_i ratios are <1 for both compounds). The prediction of the extent of

unconjugated bilirubin elevation in vivo from in vitro data is a difficult process due to uncertainty in the projection of in vivo concentrations of the inhibitor that are available to inhibit UGT1A1 and potential inaccuracies in the determination of K_i for inhibition of UGT1A1 by atazanavir and indinavir. The value for [I] should in theory be the concentration of an inhibitor at the site of UGT1A1 in the liver, which is impossible to directly measure. For drugs transported into the liver by passive diffusion, the free drug concentration in the liver probably equals that in the liver capillary artery and is always changing with a gradient formed from portal vein entrance to the hepatic vein exit (Ito et al., 1998). To be practical and to avoid false negatives caused by underestimation of the unbound drug concentrations, the maximum plasma unbound concentration, $C_{max,u,}$ is used for our estimation, which still would likely underestimate the concentration at the entrance to the liver where both blood flow from the hepatic artery and portal vein from gastrointestinal absorption contribute (Ito et al., 2002).

An elegant study by Rhame et al (2004) demonstrated that C_{min} may also contribute to hyperbilirubinemia induced by indinavir. A dose of indinavir at 667 mg in combination with ritonavir at 100 mg every 12 h produced a 6-fold increase in indinavir C_{min} (from 0.25 to 1.5 μM) as well as 1.6 fold increase in indinavir AUC_{0-24} compared to indinavir alone at 800 mg every 8 h. The indinavir C_{max} level of these two dosing regimens were comparable. The total serum bilirubin values increased with indinavir/ritonavir and indinavir alone from 0.5 and 0.7 mg/dl on day 1 to 1.2 and 0.9 mg/dl on day 14 and appeared to correlate with the increase in C_{min}. The C_{min}/K_i and $C_{min,u}/K_i$ values calculated using the K_i values determined

DMD5447

in this study are 0.03 and 0.012. Neither of them would be expected to produce significant inhibition at C_{min} (Table 5). However, this does not rule out the distinct possibility that this interaction will be dependent on inhibitor concentrations other than the C_{max} values. The kinetics of drug and inhibitor clearance will always affect the magnitude of overall effect on AUC_i/AUC and in the case where the 'drug' is an endogenous compound that is continually produced and excreted (e.g., bilirubin), the impact of inhibitor kinetics would be expected to play a major role. Although the C_{min} does not seem to explain the overall magnitude of the effects seen with atazanavir and indinavir, there may be methods that integrate the relationship of inhibitor concentration to K_i over the entire exposure window that would give better estimations of interactions caused by inhibitors of endogenous processes.

There are additional factors that could confound our capability to predict the magnitude of unconjugated bilirubin elevation from in vitro data. Many of these would be expected to be similar to those encountered when attempting to predict drug-drug interactions resulting from CYP inhibition, including selection of the most appropriate measure of in vivo inhibitor concentration (free drug vs total drug, and different inhibitor concentrations at the enzyme active site from in the circulation), and corrections of in vitro parameters due to microsomal binding. These factors have been the subject of extensive reviews (Ito et al., 1998; Thummel and Wilkinson, 1998; Bertz and Grannerman, 1997). The prediction of interactions caused by inhibition of UGT enzymes involves several additional variables (Lin and Wong, 2002; Kiang et al., 2005). These are associated with

22

DMD5447

technical limitations of in vitro glucuronidation experiments to determine K_i and may explain why the quantitative extrapolations from in vitro data to the in vivo observations remain to be validated (Remmel 2002). For UGT mediated glucuronidation reactions, Kiang et al (2005) described many cases in which potent in vitro inhibition of UGT enzymes did not correlate with in vivo effects and suggested to take cautions when using in vitro inhibition data. The in vitro experiments typically require disruption of the endoplasmic reticulum membrane by pore-forming molecules such as alamethicin to increase access of substrate and cofactor and to facilitate removal of metabolite and UDP from the lumenally localized UGT active site (Fisher et al., 2001). Non-specific binding to proteins and phospholipids has been demonstrated to decrease inhibition potency (increased apparent K_i) (Margolis and Obach, 2003). It has been reported that UGT1A1 displays allosteric binding properties for substrates and inhibitors (Rios and Tephly, 2002; Williams et al., 2002). Collectively, use of a fixed and projected inhibitor concentration, the potentially allosteric properties of UGT1A1, and sensitivity toward lipid microenvironment on bilirubin glucuronidation (Whitmer et al., 1986) may have limited our quantitative prediction of reversible hyperbilirubinemia from in vitro UGT1A1 inhibition by atazanavir and indinavir.

In summary, our in vitro data demonstrates that both atazanavir and indinavir inhibit UGT1A1 mediated bilirubin glucuronidation. The results provide a mechanism for the hyperbilirubinemia associated with administration of atazanavir as well as indinavir. We have used a variety of techniques to try to correlate the in vitro UGT1A1 inhibition parameters for a series of HIV protease

DMD5447

inhibitors to the clinical observations of hyperbilirubinemia. Our results indicate that the unbound C_{max} inhibitor concentration is a better predictor of the clinical observations than the total C_{max} plasma concentration. Future studies will be necessary to determine if this finding can be extrapolated to other UGT interactions. In addition, more studies are needed to better define how the pharmacokinetics of enzyme inhibitors influence drug-drug interactions, especially in the case of inhibition of endogenous pathways.

DMD5447

REFERENCES

Balani SK, Woolf EJ, Hoagland VL, Sturgill MG, Deutsch PJ, Yeh KC, and Lin JH (1996) Disposition of indinavir, a potent HIV-1 protease inhibitor, after an oral dose in humans. *Drug Metab Dispos* **24:**1389-1394.

Berk PD, Jones EA, and Berlin NI (1979) Disorder of bilirubin metabolism. PK Bondy and L Rosenberg, Eds. *Metabolic control and diseases*. 8th edition. Sanders, Philadelphia, P1009-1088.

Berk PD, Rodkey FL, Blaschke TF, Collison NA, and Waggoner JG (1974) Comparison of plasma bilirubin turnover and carbon monoxide production in man. *J Lab Clin Med* **83:**29-37.

Bertz RJ and Grannerman GR (1997) Use of in vitro and in vivo data to estimate the likelihood of metabolic pharmacokinetic interactions. *Clin Pharmacokinet* **32(3):** 210-258.

Boase S and Miners JO (2002) In vitro-in vivo correlations for drugs eliminated by glucuronidation: investigations with the model substrate zidovudine. *Br J Clin Pharmacol* **54:** 493-503.

Brierley C and Burchell B (1993) Human UDP-glucuronosyl transferases: chemical defense, jaundice and gene therapy. *BioEssays* **15:** 749-754.

Briz O, Serrano MA, Maclas RI, Gonzalez-Gallego J, and Marin JJ (2003) Role of organic anion-transporting polypeptides, OATP-A, OATP-C, and OATP-8, in the human placenta-maternal liver tandem excretory pathway for foetal bilirubin. *Biochem J* **371:** 897-905.

Burchell B, Brierley C, and Rance D (1995) Specificity of human UDP-glucuronosyltransferases and xenobiotic glucuronidation. *Life Sci* **57:** 1819-1831.

Campbell SD, de Morais SM, and Xu JJ (2005) Inhibition of human organic anion transporting polypeptide OATP1B1 as a mechanism of drug-induced hyperbilirubinemia. *Chem Biol Interact* **150:** 179-187.

Ciotti M, Cho J, George J, and Owens I (1998) Required buried alpha-helix structure in bilirubin UDP-glucuronosyltransferase, UGT1A1, contains a nonreplaceable phenylalanine. *Biochem* **37:** 11018-11025.

de Maat MMR, Ekhart GC, Huitema ADR, Koks CHW, Mulder JW, and Beijnen JH (2003) Drug interactions between antiretroviral drugs and comedicated agents. *Clin Pharmacokinet* **42(2):** 223-282.

Ernest II CS, Hall SD, and Jones DR (2005) Mechanism-based inactivation of CYP3A by HIV protease inhibitors. *J Pharmacol Exper Ther* **312:**583-591.

DMD5447

Fisher MB, Paine MF, Strelevitz TJ, and Wrighton SA (2001) The role of hepatic and extrahepatic UDP-glucuronosyltransferases in human drug metabolism. *Drug Metab Rev* **33:** 273-297.

Flexner C (2000) Dual protease inhibitor therapy in HIV infected patients: pharmacologic rationale and clinical benefits. *Annu Rev Pharmacol Toxicol* **40:** 649-674.

Galetin A, Ito K, Hallifax D, and Houston JB (2005) CYP3A4 substrate selection and substitution in the prediction of potential drug-drug interaction. *J Pharmacol Exper Ther* **314:** 186-190.

Goldsmith DR and Perry CM (2003) Atazanavir. *Drugs* **63:**1679-1693.

Green MD, King CD, Mojarrabi B, Mackenzie PI, and Tephly TR (1998) Glucuronidation of amines and other xenobiotics catalyzed by expressed human UDP-glucuronosyltransferase 1A3. *Drug Metab Dispos* **26:** 507-512.

Hurst M and Faulds D (2000) Lopinavir. *Drugs* **60:** 371-1379.

Ito K, Chiba K., Horikawa M, Ishigami M, Mizuno N, Aoki J, Gotoh Y, Iwatsubo T, Kanamitsu S, Kato M, Kawahara I, Niinuma K, Nishino A, Sato N, Tsukamoto Y, Ueda K, Itoh T, and Sugiyama Y (2002) Which concentration of the inhibitor should be used to predict in vivo drug interactions from in vitro data ? *AAPS PharmaSci* **4:** 1-8.

Ito K, Hayley SB, and Houston JB (2004) Database analyses for the prediction of in vivo drug-drug interactions from in vitro data. *Br J Clin Pharmacol* **57:** 473-486.

Ito K, Iwatsubo T, Kanamitsu S, Ueda K, Suzuki H, and Sugiyama Y (1998) Prediction of pharmacokinetic alerations caused by drug-drug interactions: Metabolic interaction in the liver. *Pharmacol Rev* **50:** 387-411.

Ito K, Obach RS, and Houston JB (2005) Impact of parallel pathways of drug elimination and multiple CYP involvement on drug-drug interactions: CYP2D6 paradigm. *Drug Metab Dispos* **33:** 837-844.

Kamisako T, Kobayashi Y, Takeuchi K, Ishihara T, Higuchi K, Tanaka Y, Gabazza EC, and Adachi Y (2000) Recent advances in bilirubin metabolism research: molecular mechanism of hepatocyte bilirubin transport and its clinical relevance. *J Gastroenterol* **35:** 659-664.

Keppler D and Konig CJ (2000) Hepatic secretion of conjugated drugs and endogenous substances. *Semin Liver Dis* **20:** 265-272.

Kiang TKL, Ensom MHH, and Chang TKH (2005) UDP-glucuronosyltransferases and clinical drug-drug interactions. *Pharmacol Ther* **106:** 97-132.

DMD5447

Kuehl GE, Lampe JW, Potter JD, and Bigler J (2005) Glucuronidation of nonsteroidal anti-inflammatory drugs: identifying the enzymes responsible in human liver microsomes. *Drug Meta Dispos* **33:** 1027-1035.

Lin JH and Wong BK (2002) Complexities of glucuronidation affecting in vitro-in vivo extrapolation. *Curr Drug Metab* **3:** 623-646.

Liston HL, Markowitz JS, and Devane CL (2001) Drug glucuronidation in clinical psychopharmacology. *J Clin Psychopharmacol* **21:** 500-515.

Luukkanen L, Taskinen J, Kurkela M, Kostiainen R, Hiruonen J, and Finel M (2005) Kinetic characterization of 1A family of recombinant human UDP-glucuronosyltransferases. *Drug Metab Dispos* **33:** 1017-1026.

Margolis JM and Obach RS (2003) Impact of nonspecific binding to microsomes and phospholipids on the inhibition of cytochrome P4502D6: Implications for relating in vitro inhibition data to in vivo drug interactions. *Drug Metab Dispos* **31:** 606-611.

McPhee F, Caldera PS, Bemis GW, McDonagh AF, Kuntz ID, and Craik CS (1996) Bile pigments as HIV-1 protease inhibitors and their effects on HIV-1 viral maturation and infectivity in vitro. *Biochem J* **320:** 681-686.

Miners JO, McKinnon RA, and Mackenzie PI (2002) Genetic polymorphisms of UDP-glucuronosyltransferases and their functional significance. *Toxicol* **181–182:** 453-456.

Miners JO, Smith PA, Sorich MJ, McKinnon RA, and Mackenzie PI (2004) Predicting human drug glucuronidation parameters: application of in vitro and in silico modeling approaches. *Annu Rev Pharmacol Toxicol* **44:** 1-25.

Odell G, Mogilevsky WS, and Gourley (1990) High-performance liquid chromatographic analysis of bile pigments as their native tetrapyrroles and as their dipyrrolic azosulfanilate derivatives. *J Chromatography* **529:** 287-298.

O'Mara EM, Mummaneni V, Burchell B, Randall D, Geraldes M (2000) Relationship between uridine diphosphate-glucuronosyltransferase (UDP-GT) 1A1 genotype and total bilirubin elevations in healthy subjects receiving BMS-232632 and saquinavir. *40th Interscience Conference on Antimicrob Agent Chemother* Abst 1645.

Remmel RP (2002) In Drug-Drug Interactions (Rodrigues AD ed.) Marcel Dekker, NY, p89-121.

Rhame FS, Rawlins SL, Petruschke RA, Erb TA, Winchell GA, Wilson HM, Edelman JM, and Abramson MA (2004) Pharmacokinetics of indinavir and ritonavir administration at 667 and 100 milligrams, respectively, every 12 hours compared with indinavir administered 800 milligrams every 8 hours in human immunodeficiency virus-infected patients. *Antimicrob Agent Chemother* **48:** 4200-4208.

DMD5447

Rios GR and Tephly TR (2002) Inhibition and active sites of UDP-glucuronosyltransferases 2B7 and 1A1. *Drug Metab Dispos* **30:** 1364-1367.

Rodrigues AD, Winchell GA, and Dobrinska MR (2001) Use of in vitro drug metabolism data to evaluate metabolic drug-drug interactions in man: the need for quantitative databases. *J Clin Pharmacol* **41:** 368-373.

Rowland M and Matin SB (1973) Kinetics of drug-drug interactions. *J Pharmacokinet Biopharm* **1:**553-567.

Segel IH (1993) Enzyme Kinetics, Wiley-Interscience Publication, N.Y.

Senafi S, Clarke D, and Burchell B (1994) Investigation of the substrate specificity of a cloned expressed human bilirubin UDP-glucuronosyltransferase: UDP-sugar in steroid and xenobiotic glucuronidation. *Biochem J* **303:** 233-240.

Sulkowski MS (2004) Drug-induced liver injury associated with antiretroviral therapy that includes HIV-1 protease inhibitors. *Clin Infect Dis* **38:** S90-97.

Tachibana M, Tanaka M, Masubuchi Y, and Horie Y (2005) Acyl glucuronidation of fluoroquinolone antibiotics by the UDP-glucuronosyl transferase 1A subfamily in human liver microsomes. *Drug Metab Dispos* **33:**803-811.

Thummel KE and Wilkinson GR (1998) In vitro and in vivo drug interactions involving human CYP3A. *Ann Rev Pharmacol Toxicol* **38:**389-430.

Tukey RH and Strassburg CP (2000) Human UDP-glucuronosyltransferases: Metabolism, expression, and disease. *Annu Rev Pharmacol Toxicol* **40:** 581-616.

Venkatakrishnan K, von Moltke LL, and Greenblatt DJ (2001) Human drug metabolism and the cytochromes P450: Application and relevance of in vitro models. *J Clin Pharmacol* **41:**1149-1179.

Williams JA, Hyland R, Jones BC, Smith DA Hurst S, Goosen TC, Peterkin V, Koup JR, and Ball SE (2004) Drug-drug interactions for UDP-glucuronosyltransferase substrates: A pharmacokinetic explanation for typically observed low exposure (AUCi/AUC) ratios. *Drug Metab Dispos* **32:** 1201-1208.

Williams JA, Ring BJ, Cantrell VE, Campanale K, Jones DR, Hall SD, and Wrighton SA (2002) Differential modulation of UDP-glucuronosyltransferase 1A1 (UGT1A1)-catalyzed estradiol-3-glucuronidation by the addition of UGT1A1 substrates and other compounds to human liver microsomes. *Drug Metab Dispos* **30:** 1266-1273.

Whitmer DI, Russell PE, Ziurys JC, and Gollan JL (1986) Hepatic microsomal glucuronidation of bilirubin is modulated by the lipid microenvironment of membrane-bound substrate. *J Biol Chem* **261:**7170-7177.

DMD5447

Yao C and Levy RH (2002) Inhibition-based metabolic drug-drug interactions: predictions from in vitro data. *J Pharm Sci* **91:** 1923-1935.

Zucker S, Qin X, Rouster S, Yu F, Green R, Keshavan P, Feinberg J, and Sherman KE (2001) Mechanism of indinavir-induced hyperbilirubinemia. *Proc Natl Acad Sci USA* **98:**12671-12676.

DMD5447

Figure Legends

Figure 1. Structures of HIV protease inhibitors

Figure 2. Bilirubin glucuronidation by UGT1A1

Figure 3. HPLC chromatogram of an *in vitro* bilirubin glucuronidation reaction catalyzed by human UGT1A1. Bilirubin di-glucuronide eluted at 12.5 min and the peaks eluting between 15.4 and 16.6 min are bilirubin mono-glucuronide isomers. Bilirubin and glucuronide metabolites were detected at 450 nm.

Figure 4. (A) Lineweaver-Burke plot (1/V vs. 1/[S]) of substrate concentration dependence of bilirubin glucuronidation in the presence of fixed concentrations of atazanavir (inhibitor). Bilirubin concentrations were 3, 6, 9, 12, and 15 μM. (B) Re-plot of the slopes and y-intercepts from the double-reciprocal plot vs the inhibitor, atazanavir. The x-intercept of the slope re-plot is equal to $-K_i$ (1.9 μM). The x-intercept of the y-intercept re-plot is equal to $-\alpha K_i$ (16.4 μM).

Figure 5. A Dixon plot of bilirubin glucuronidation in the presence of fixed concentrations of atazanavir (inhibitor).

Figure 6. (A) Lineweaver-Burke plot (1/V vs. 1/[S]) of bilirubin glucuronidation in presence of increasing concentrations of indinavir. Bilirubin concentrations were 2, 5, 10, and 20 μM. (B) Re-plot of the slopes and y-intercepts from the double-reciprocal plot vs the inhibitor indinavir. The x-intercept (K_i) of slope vs. [I] equals 47.9 μM. The x-intercept (αK_i) of y-intercept vs. [I] equals 1317 μM.

30

Table 1: UGT enzyme assays for determination of IC$_{50}$ values of HIV protease inhibitors

Enzyme[1]	Substrates	[Subs][5] (µM)	Analytical Standard	Detection (nm)	Control Inhibitors	[Inhibitor] (µM)	Percent inhibition
UGT1A1[2]	Bilirubin	5	Bilirubin	450	β-Estradiol	200	61.5
UGT1A3[3]	β-Estradiol	40	β-Estradiol glucuronide	280	2-Hydroxy-estradiol	100	38.5
UGT1A4[4]	Trifluoperazine	60	Trifluoperazine	256	Hecogenin	50	48.0
UGT1A6[4]	HFC[6]	50	HFC glucuronide	325	Naphthol	50	87.0
UGT1A9[4]	HFC	10	HFC glucuronide	325	Propofol	50	37.0
UGT2B7[4]	HFC	50	HFC glucuronide	325	Eugenol	100	54.5

[1] Human cDNA-expressed UGT1A1 in baculovirus infected insect cells.

[2] Buffer=50 mM Na citrate, pH 7.5; enzyme proteins=0.2 mg/ml; time=30 min.

[3] Buffer=50 mM Tris-HCl, pH 7.5; enzyme proteins=1 mg/ml; time=30 min.

[4] Buffer=50 mM Tris-HCl, pH 7.5; enzyme proteins=0.4 mg/ml; time=20 min (except 10 min for UGT1A6).

[5] Literature apparent K$_m$ values are 5, 39, 61, 321, 2.3, and 161 µM, respectively, for these reactions.

[6] HFC=7-Hydroxy trifluoromethyl coumarin.

31

DMD5447

Table 2: IC_{50} determination for inhibition of UGTs by HIV protease inhibitors

HIV Inhibitor	IC_{50} Values (μM)[1]					
	UGT1A1	UGT1A3	UGT1A4	UGT1A6	UGT1A9	UGT2B7
Atazanavir	2.3	7.9	21	>100	>100	>100
Indinavir	87[2]	26	>100	>100	>100	>100
Saquinavir	13	5.5	8.0	>100	>100	>100
Lopinavir	8.6	3.9	7.6	>100	>100	>100
Ritonavir	19	6.3	2.0	>100	>100	>100
Nelfinavir	11	60	55	>100	>100	>100

[1] Human cDNA-expressed UGT1A1 in baculovirus-infected insect cells.

[2] The value was 87 μM from a determination in cDNA-expressed UGT1A1 in lymphoblast cells as described in Table 3. The IC_{50} value was 111 μM from the determination in cDNA-expressed UGT1A1 in baculovirus- infected insect cells.

DMD5447

Table 3: IC$_{50}$ determinations and K$_i$ estimation for the inhibition of bilirubin glucuronidation in HLM and cDNA-expressed UGT1A1

HIV Inhibitor	IC$_{50}$ Values (μM)[2]		K$_i$ Estimates (μM)[3]	
	UGT1A1	HLM	UGT1A1	HLM
Atazanavir	2.4	2.5	1.2	1.3
Indinavir	87	68	44	34
Saquinavir	7.3	5.0	3.7	2.5
Nelfinavir	8.4	2.7	4.2	1.4

[1] Human cDNA-expressed UGT1A1 in lymphoblast cells.

[2] Positive control was β-estradiol (UGT1A1).

[3] K$_i$ was estimated based on K$_i$=1/2 x IC$_{50}$ when [S]=K$_m$, assuming a competitive inhibition.

DMD5447

Table 4: Summary of inhibition kinetics of UGT1A1 bilirubin glucuronidation by atazanavir and indinavir

$$E + S \underset{Km}{\rightleftharpoons} ES \xrightarrow{Kcat} E + P$$

$$V = \frac{V\max[S]}{Km(1+\frac{[I]}{Ki})+[S](1+\frac{[I]}{\alpha Ki})}$$

$E + I \quad\quad ES + I$

$Ki \updownarrow \quad\quad \alpha Ki \updownarrow$

$EI \quad\quad ESI$

$$V\max = Kcat[E_o]$$

$E = UGT \quad\quad S = Bilirubin$

$I = BMS\text{-}232632 \text{ or } Indinavir$
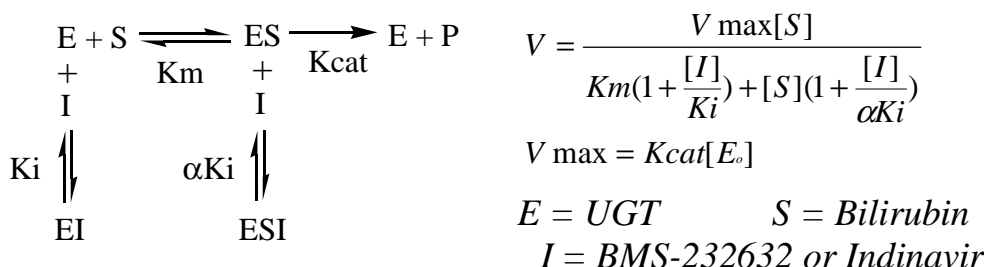
HIV Inhibitor	K_i (µM)	αK_i (µM)	Inhibition Mechanism	Predicted Inhibition at C_{ss}[5]
Atazanavir[2]	1.9	16.4 (α =8.6)	Linear Mixed	28.7%
Indinavir[3]	47.9	1317 (α =27.5)	Linear Mixed[4]	2.5%

[1] Human cDNA-expressed UGT1A1 in lymphoblast cells.

[2] UGT 1A1: Apparent K_m = 4 µM and V_{max} = 80 pmol/min mg protein in this set of experiments.

[3] UGT 1A1: Apparent K_m = 2.8 µM and V_{max} = 62 pmol/min mg protein in this set of experiments.

[4] An uncompetitive mechanism with a K_i = 100 µM was reported (FDA Summary Basis of Approval-indinavir).

[5] For atazanavir, C_{ss} = 1.73 µM (400 mg QD); for indinavir, C_{ss} = 3.84 µM (Crixivan package insert, 800 mg TID); [Bilirubin] = 6.84 µM.

Table 5: Relationship of UGT1A1 inhibition and occurrence of hyperbilirubinemia by HIV protease inhibitors

HIV Inhibitor	Dose (mg)	$F_u{}^2$	C_{max} - $C_{min}{}^2$ (μM)	$C_{max,u}$ - $C_{min,u}{}^2$ (μM)	K_i (μM)	C_{max}/K_i - $C_{min}/K_i{}^4$	$C_{max,u}/K_i$ - $C_{min,u}/K_i{}^4$	Observed Hyper-bilirubinemia[5]
Atazanavir	400 QD	0.135	6.28-0.312	0.847-0.042	1.9	3.31-0.16	0.45-0.02	Yes, some patients
Indinavir	800 TID	0.40	12.6-0.293	5.04-0.117	47.9	0.26-0.06	0.11-0.002	Yes, some patients
Saquinavir	600 TID	<0.02	0.29-0.060	0.006-0.001	6.52[3]	0.04-0.01	0-0	No
Lopinavir[1]	400 BID	<0.02	15.3-8.75	0.306-0.175	4.3[3]	3.56-2.03	0.07-0.04	No
Ritonavir	600 TID	<0.02	15.6-5.15	0.312-0.103	9.5[3]	1.64-0.54	0.03-0.01	No
Nelfinavir	750 TID	<0.02	6.70-2.44	0.134-0.049	5.5[3]	1.22-0.44	0.02-0.01	No

[1] The combination of lopinavir and ritonavir (400 mg/100 mg) was approved for clinical use (Hurst and Faulds, 2000).

[2] Plasma protein unbound drug fraction F_u, maximum plasma drug concentration (C_{max}), and plasma drug concentration at trough (C_{min}) values were from literature reports (Goldsmith and Perry, 2003; Flexner, 2000; de Maat et al., 2003). Free drug concentrations were calculated by multiplying drug concentrations by F_u.

[3] K_i was estimated based on $K_i = 1/2 \times IC_{50}$ when [S]=K_m, assuming a competitive inhibition.

[4] $AUC_i/AUC = 1 + [I]/K_i$ (Ito et al., 1998); [I] = C_{max}, C_{min}, $C_{max,u}$, or $C_{min,u}$ for prediction.

[5] Elevated unconjugated bilirubin was associated with administration of atazanavir and indinavir in some patients (Goldsmith and Perry, 2003; Flexner, 2000)
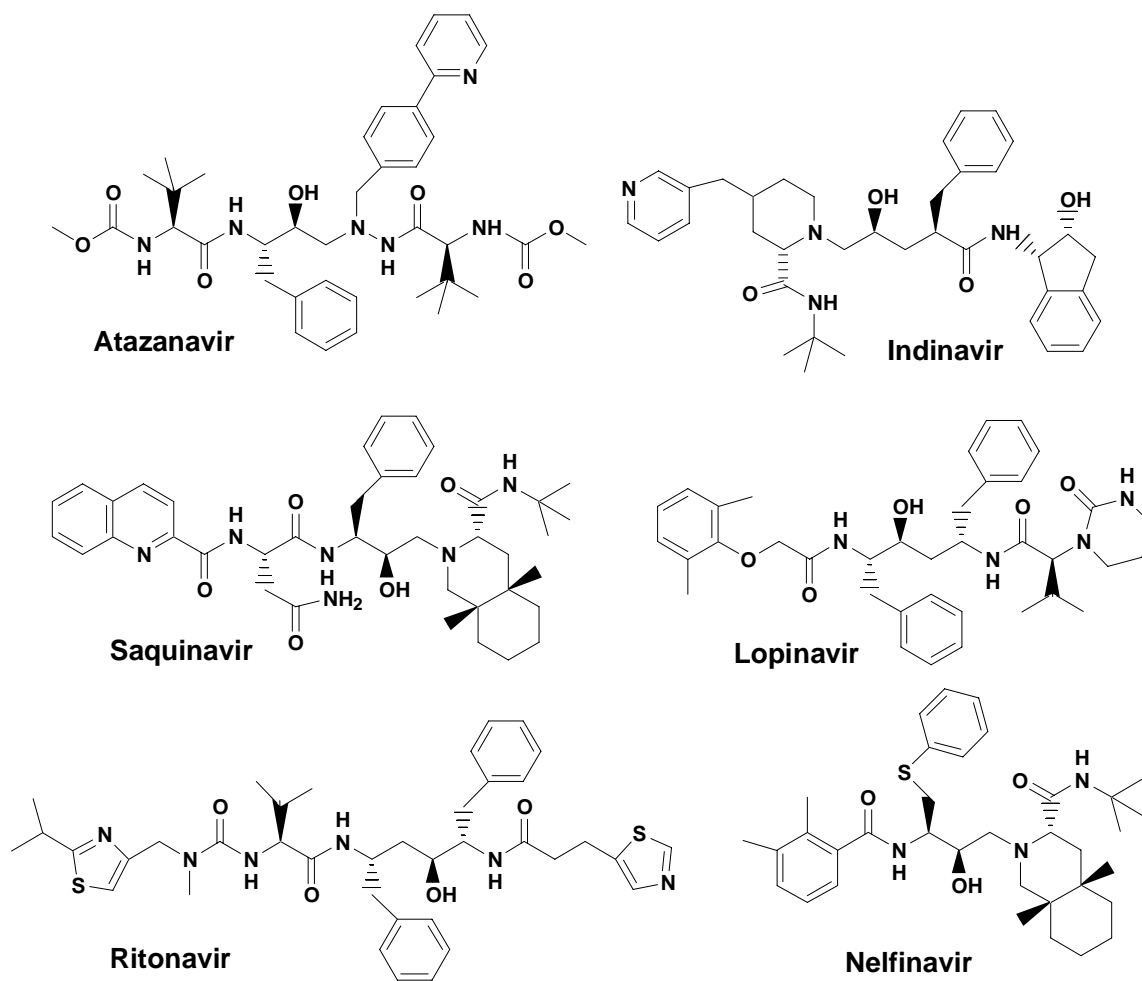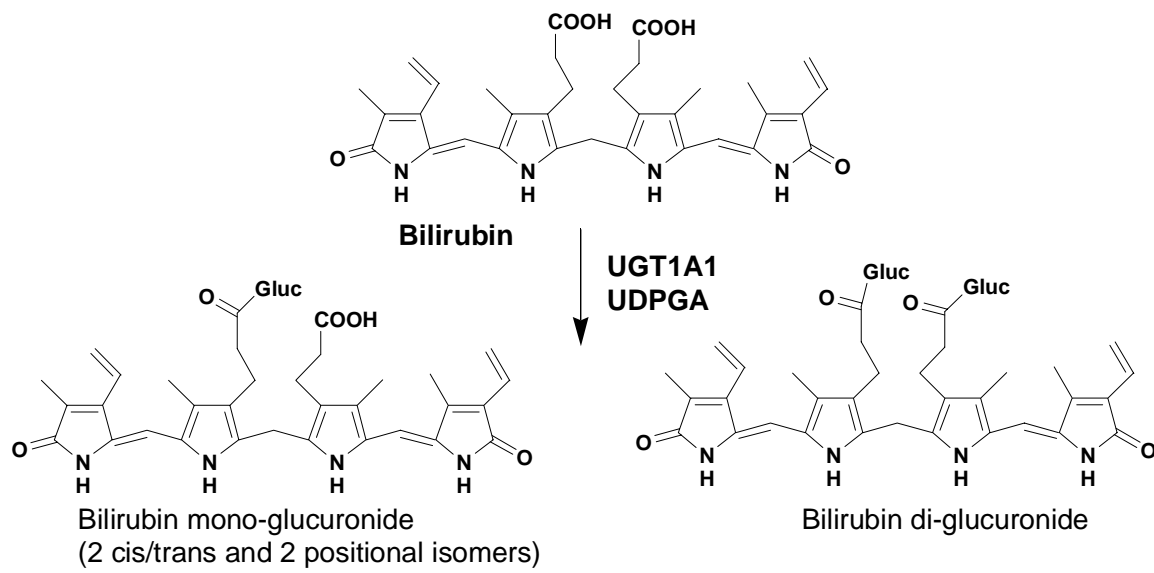
Fig. 1

Atazanavir
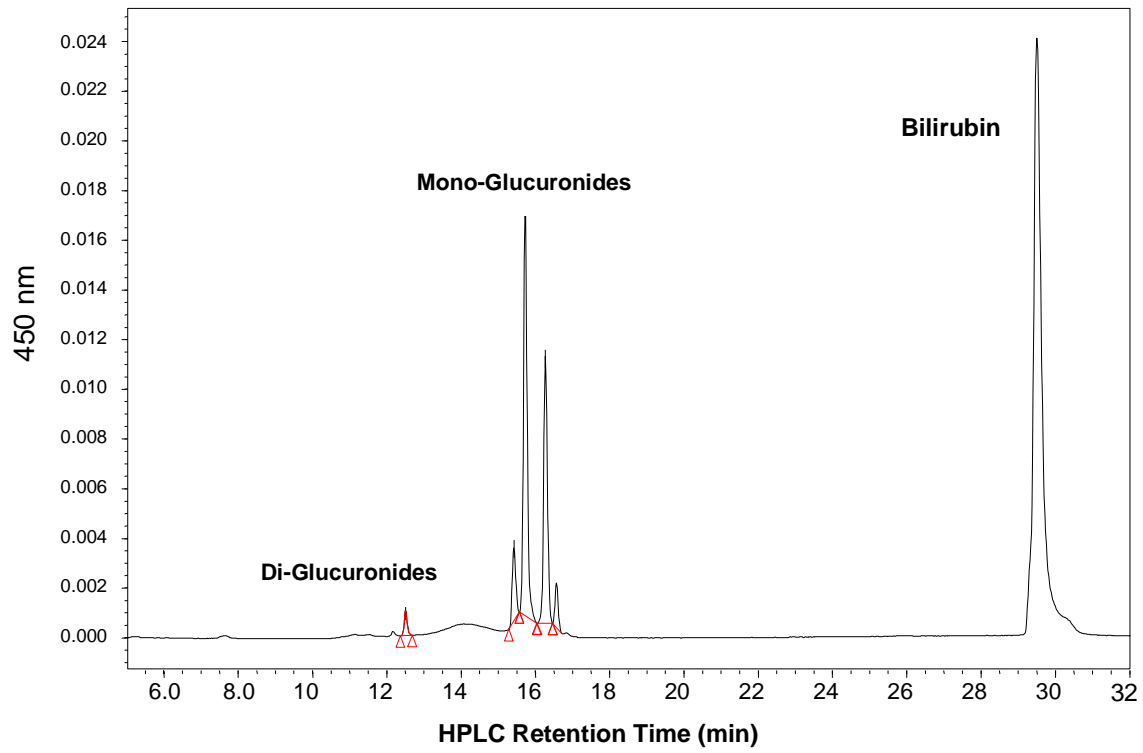
Indinavir

Saquinavir

Lopinavir

Ritonavir

Nelfinavir

Fig. 2

Bilirubin

UGT1A1
UDPGA

Bilirubin mono-glucuronide
(2 cis/trans and 2 positional isomers)

Bilirubin di-glucuronide

Fig. 3

Fig. 4

Fig. 5

Fig. 6